

AD-A193 387

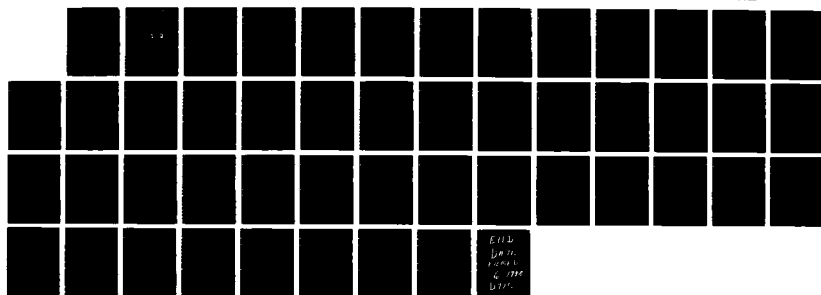
THE INFLUENCE OF SURFACE ROUNDING ON TRAILING EDGE
NOISE(U) BBN LABS INC CAMBRIDGE MA M S HOWE JAN 88
BBN-6715 W00167-87-C-0021

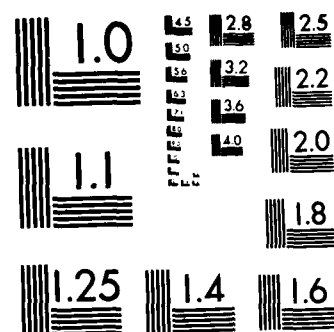
1/1


UNCLASSIFIED

F/G 20/1

NL






 MICROCOPY RESOLUTION TEST CHART
 NATIONAL BUREAU OF STANDARDS-1963-A

BBN Laboratories Incorporated

A Subsidiary of Bolt Beranek and Newman Inc.

DTIC FILE COPY 4

Report No. 6715

AD-A193 387

THE INFLUENCE OF SURFACE ROUNDING ON TRAILING EDGE NOISE

M.S. Howe

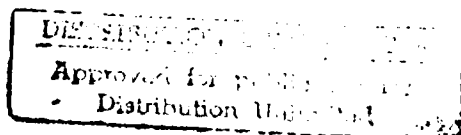
January 1988

DTIC
ELECTE
MAR 30 1988
S α D

Contract No.: N00167-87-C-0021

Prepared by:

BBN Laboratories Incorporated
10 Moulton Street
Cambridge, MA 02238



Prepared for:

Office of Naval Research
Applied Hydrodynamics Research Program
Arlington, VA 22217
Attention: James A. Fein

88 1 27 165

Report No. 6715

THE INFLUENCE OF SURFACE ROUNDING ON TRAILING EDGE NOISE

M.S. Howe

January 1988

Contract No.: N00167-87-C-0021

Prepared by:

BBN Laboratories Incorporated
10 Moulton Street
Cambridge, MA 02238

Prepared for:

Office of Naval Research
Applied Hydrodynamics Research Program
Arlington, VA 22217
Attention: James A. Fein

Accession For	
NTIS CRA&I	<input checked="checked" type="checkbox"/>
DTIC TAB	<input type="checkbox"/>
Unannounced	<input type="checkbox"/>
Justification	
By <i>per ltr</i>	
Distribution	
Availability Codes	
Dist	Avail and for Special
A-1	



SUMMARY

An analysis is made of the sound produced by low Mach number turbulent flow over an asymmetrically rounded trailing edge of an airfoil. Such airfoils are used in experimental studies of trailing edge noise and vortex shedding phenomena, and have a flat pressure side and a rounded, or "beveled", suction surface at the trailing edge, so that in the immediate vicinity of the edge the airfoil has a wedge shaped profile. There are two principal interaction noise sources: a lift dipole associated with the unsteady transverse forces exerted on the airfoil, and a thickness dipole which radiates preferentially in the plane of the airfoil. The latter is usually negligible except possibly at low frequencies, and at large included angles of the trailing edge wedge. Detailed results are given for included angles of 90° and less. It is concluded that, for given turbulence intensity, surface beveling has a significant effect on the radiation only at sufficiently high frequencies that the trailing edge may be regarded as a straight-sided wedge over distances of the order of the turbulence length scale.

TABLE OF CONTENTS

	page
SUMMARY.....	ii
SECTION 1. INTRODUCTION.....	1
2. THE AERODYNAMIC SOUND PROBLEM.....	4
2.1 Formulation and General Solution.....	4
2.2 The Lift and Thickness Components of the Diffraction Radiation.....	7
3. THE ACOUSTIC GREEN'S FUNCTION FOR SOURCES NEAR THE TRAILING EDGE.....	10
3.1 Evaluation of $Y_2(\underline{x})$	10
3.2 Evaluation of $\phi_f^*(\underline{x})$	14
4. NOISE PRODUCED BY TURBULENCE ON THE PRESSURE SIDE OF THE AIRFOIL.....	17
4.1 The Lift Dipole $p_2(\underline{x},t)$	17
4.2 The Thickness Dipole $p_1(\underline{x},t)$	21
5. THE KUTTA CONDITION.....	22
5.1 The Green's Function $G(\underline{x},\underline{y},t,\tau)$ for <u>x</u> Near the Trailing Edge.....	22
5.2 Induced Flow Near the Edge.....	25
5.3 The Shed Vorticity.....	26
6. THE RADIATED SOUND.....	28
6.1 The Acoustic Pressure Spectra.....	28
6.2 The Boundary Layer Turbulence.....	31
6.3 Numerical Results.....	34
7. DISCUSSION OF THE GENERAL CASE.....	39
7.1 Turbulence on the Suction Surface.....	39
7.2 Influence of Non-Compactness.....	40
8. CONCLUSION.....	43
REFERENCES.....	44

1. INTRODUCTION

Sound is produced when turbulence is convected in mean flow over the trailing edge of an airfoil [1-4]. The strength of the radiation is governed by the relative magnitudes of the turbulence length scale and the radius of curvature of the edge, such that for given turbulence intensity, it attains a maximum when the turbulence scale is large relative to the thickness of the edge. An edge of blunted or rounded profile cannot always be used to reduce trailing edge noise, however, because of the tendency of the flow to separate and produce increased turbulence levels. In addition, separation is often accompanied by the quasi-periodic shedding of large spanwise vortices, which are coherent over distances equal to several edge thicknesses, and can induce harmful, large amplitude structural vibrations together with a strong tonal component of the radiated sound ("hydrofoil singing") [5].

Blake and co-workers [5,6] have undertaken extensive experimental investigations to clarify the role of trailing edge geometry on singing, structural vibration and the broadband radiated sound. Of particular interest in these studies is the configuration depicted in Figure 1, in which the trailing edge is asymmetrically "beveled", i.e., such that the suction side of the airfoil is rounded at the trailing edge and intersects a plane pressure side at a finite included angle $\bar{\theta}$. Separation does not occur provided $\bar{\theta}$ is less than about 30° , except possibly at very high mean flow velocities. Although the edge is sharp, it might be expected that the intensity of the edge noise will be reduced compared to that produced by an edge of zero included angle, provided the frequency is large enough that the edge may be regarded as a straight-sided wedge of angle $\bar{\theta}$ over distances of the order of the turbulence length scale (c.f., [7]).

In this paper a theoretical investigation is made of the influence of asymmetric beveling on the broadband component of the edge noise produced by turbulent boundary layer flow over the trailing edge region. The analysis is performed for included angles in the range $0 < \bar{\theta} < 90^\circ$. Periodic vortex shedding will in practice occur at the larger values of $\bar{\theta}$, but this will not be discussed explicitly. In a first approximation its influence will be to contribute an additional tonal peak to the broadband spectrum of the predicted radiation. The results are used to deduce a simple formula which provides the correction due to beveling of the trailing edge noise that would be predicted for the ideal case of an airfoil modeled by a flat plate of infinitesimal thickness [4].

The edge noise can be ascribed to a distribution of dipole sources on the surface of the airfoil whose axes are in the direction of the local normal to the surface. In the case of an airfoil of finite thickness some of these dipoles are aligned with the mean flow, into which direction they radiate preferentially. This thickness effect is absent in the conventional theory of trailing edge noise [4], which associates the principal sources of sound with dipoles orientated at right angles to the flow, i.e., to fluctuations in the lift of the airfoil. For an asymmetrically beveled edge it will be shown that the thickness component of the radiation is likely to be significant only for large values of the included angle $\bar{\theta}$, and when the thickness of the turbulent boundary layer at the trailing edge is greater than that of the airfoil. Detailed analytical results will be worked out for a two-dimensional airfoil of compact chord. The modifications necessary for dealing with a non-compact airfoil are briefly summarized. In both cases the Kutta condition, that the unsteady pressure and velocity should be finite at the sharp edge of the airfoil, is imposed.

In Section 2 the aerodynamic sound problem is formulated and solved by use of a Green's function for an airfoil of compact chord. The analytical structure of the Green's function for sources in the vicinity of the rounded trailing edge is determined in Section 3. Sections 4 through 6 then treat the particular case of turbulence noise sources in the boundary layer on the pressure side of the airfoil. The convection of turbulence into the trailing edge region causes additional vorticity to be shed from the edge, the magnitude of which is estimated in Section 5 by application of the unsteady Kutta condition. The shed vorticity also generates sound, and formulae for the net acoustic radiation are obtained in Section 6.

In Section 7 the general case of arbitrary turbulent flow over the trailing edge is briefly discussed, including the influence of separation and periodic vortex shedding, and the modifications necessary for dealing with an airfoil of non-compact chord.

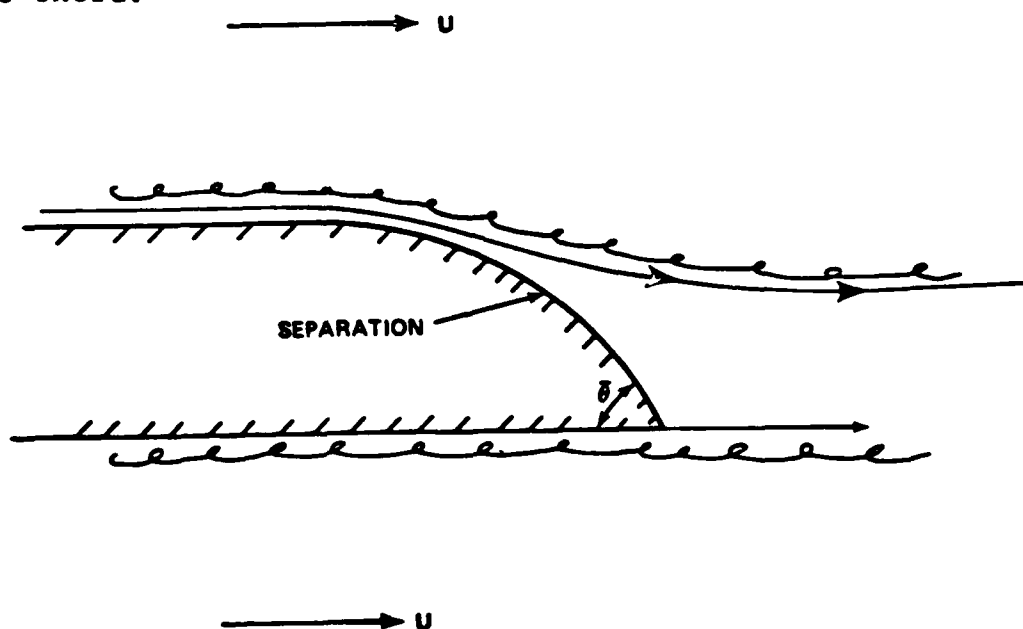


FIGURE 1. TURBULENT BOUNDARY LAYER FLOW OVER AN ASYMMETRICALLY BEVELED TRAILING EDGE. SEPARATION OCCURS TYPICALLY FOR $\theta \geq 30^\circ$.

2. THE AERODYNAMIC SOUND PROBLEM

2.1 Formulation and General Solution

Consider the generation of sound by high Reynolds number, low Mach number mean flow over the two-dimensional rigid airfoil illustrated in Figure 2. The fluid has mean density ρ_0 , sound speed c , and main stream velocity U in the positive x_1 -direction of the rectangular coordinate system (x_1, x_2, x_3) , where $M = U/c \ll 1$. The airfoil has chord $2a$ and, except in the vicinities of the leading and trailing edges, uniform thickness s , and is set at zero angle of attack to the mean flow. The upper ("suction") and lower ("pressure") surfaces of the airfoil are defined respectively by

$$\left. \begin{aligned} x_2 &= \sigma(x_1) > 0, \\ x_2 &= -0, \end{aligned} \right\} -2a < x_1 < 0, \quad (2.1)$$

where the origin of coordinates is taken at 0 at the trailing edge, and the x_3 -axis is directed out of the plane of the paper in the figure.

The boundary layers on the surfaces of the airfoil are assumed to become turbulent towards the trailing edge (and separation may also occur), and it is required to determine the sound produced by diffraction when the hydrodynamic turbulence pressure field is swept past the trailing edge region by the mean flow. The formal solution of this problem is determined by that of the inhomogeneous wave equation

$$\left. \begin{aligned} \{\partial^2/c^2\partial t^2 - \nabla^2\}B &= Q(\underline{x}, t) \\ Q(\underline{x}, t) &= \text{div}(\underline{w} \wedge \underline{v}), \end{aligned} \right\} \quad (2.2)$$

provided the Mach number M is sufficiently small that convection of sound by the mean flow can be neglected [8]. In this equation t denotes time and B is the perturbation stagnation enthalpy

$$B = p/\rho_0 + \frac{1}{2}(v^2 - U^2) , \quad (2.3)$$

where \underline{v} is the velocity, $\underline{\omega} = \text{curl } \underline{v}$ is the vorticity, and p the perturbation pressure. Sound generation by the flow is associated with those regions in which $\underline{\omega} \neq 0$. It follows from the momentum equation

$$\partial \underline{v} / \partial t + \nabla B = -\underline{\omega} \wedge \underline{v} , \quad (2.4a)$$

that elsewhere in the flow we can write

$$B = -\partial \phi / \partial t, \quad (\underline{\omega} = 0) , \quad (2.4b)$$

where $\nabla \phi$ is equal to the perturbation velocity. In particular, $B = p/\rho_0$ in the acoustic far field when $M \ll 1$.

Equation (2.2) is used to express B in terms of the vortical source Q , whose properties are assumed to be known or easily determined. This can be effected by introducing a Green's function $G(\underline{x}, \underline{y}, t, \tau)$, which is the solution of (2.2) when the right hand side is replaced by the impulsive point source $\delta(\underline{x} - \underline{y})\delta(t - \tau)$. It must satisfy the radiation condition of outgoing waves at large distances and have vanishing normal derivative $\partial G / \partial x_n$ on the surface of the airfoil. Routine application of Green's theorem [9] then yields

$$B = \int Q(\underline{y}, \tau) G(\underline{x}, \underline{y}, t, \tau) d^3 \underline{y} d\tau , \quad (2.5)$$

where the volume integral with respect to \underline{y} is taken over the region occupied by the fluid.

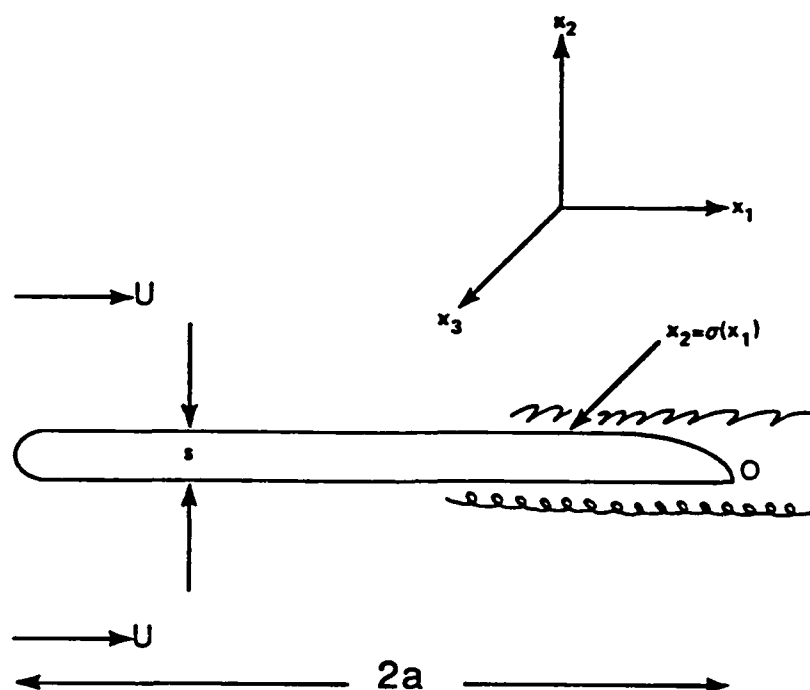


FIGURE 2. CONFIGURATION OF THE AERODYNAMIC SOUND PROBLEM.

In flow of very small Mach number the wavelength of the turbulence generated sound is much greater than the chord $2a$ of the airfoil, and to simplify the present discussion this will be assumed to be the case. Necessary modifications to deal with the non-compact airfoil are sketched-in in Section 7. In these circumstances, the radiation received at \underline{x} in the acoustic far field is determined by the low frequency or compact form of the Green's function [8] given by

$$G(\underline{x}, \underline{y}, t, \tau) = \frac{1}{4\pi |\underline{x} - \underline{y}|} \delta\{t - \tau - |\underline{x} - \underline{y}|/c\} , \quad (2.6)$$

where

$$\left. \begin{aligned} Y_i &= y_i + \phi_i^*(y) , & i &= 1, 2, \\ Y_3 &= y_3 , \end{aligned} \right\} \quad (2.7)$$

and $\phi_i^*(\underline{y}) \equiv \phi_i^*(y_1, y_2)$ is a solution of Laplace's equation $\nabla^2 \phi_i^* = 0$, which vanishes at large distances from the airfoil, and is such that the normal derivative $\partial Y_i / \partial y_n = 0$ on the surface of the airfoil. Accordingly, $Y_i(\underline{y})$ may be interpreted as the velocity potential of incompressible, irrotational flow past the airfoil which has unit speed in the i -direction at large distances from the airfoil. The approximation (2.6) is appropriate provided that the principal components of the radiation arise from the interaction of the turbulence with the airfoil, which is the case at low Mach number [10].

2.2 The Lift and Thickness Components of the Diffraction Radiation

Since $B = p/\rho_0$ in the acoustic region, equations (2.5), (2.6) imply that

$$p(\underline{x}, t)/\rho_0 = \frac{1}{4\pi} \int \frac{Q(\underline{y}, t - |\underline{x} - \underline{y}|/c) d^3 \underline{y}}{|\underline{x} - \underline{y}|} . \quad (2.8)$$

To use this result to calculate the spectral characteristics of the radiation it is convenient to introduce a Fourier integral representation of p . The Fourier transform $\hat{p}(\underline{x}_2, \underline{k}, \omega)$ of $p(\underline{x}, t)$ satisfies the following reciprocal relations

$$\hat{p}(\underline{x}_2, \underline{k}, \omega) = \frac{1}{(2\pi)^3} \int_{-\infty}^{\infty} p(\underline{x}, t) e^{-i(\underline{k} \cdot \underline{x} - \omega t)} d\underline{x}_1 d\underline{x}_3 dt , \quad (2.9a, b)$$

$$p(\underline{x}, t) = \int_{-\infty}^{\infty} \hat{p}(\underline{x}_2, \underline{k}, \omega) e^{-i(\underline{k} \cdot \underline{x} - \omega t)} d\underline{k}_1 d\underline{k}_3 d\omega ,$$

where the wavenumber vector $\underline{k} = (k_1, 0, k_3)$ has components k_1, k_3 respectively conjugate to x_1, x_3 .

Taking the Fourier transform of (2.8) and using the identity

$$\frac{e^{ik_0|\underline{x}-\underline{y}|}}{|\underline{x}-\underline{y}|} = \frac{i}{2\pi} \int_{-\infty}^{\infty} \frac{\exp[i\{\underline{k} \cdot (\underline{x}-\underline{y}) + \gamma(k)|\underline{x}_2-\underline{y}_2|\}] d^2\underline{k}}{\gamma(k)} \quad (2.10)$$

where $k_0 = \omega/c$ is the acoustic wavenumber (in terms of which sound of radian frequency ω has wavelength $2\pi/k_0$), and $\gamma(k) = \text{sgn}(k_0)|k_0^2 - k^2|^{1/2}$, $i|k_0^2 - k^2|^{1/2}$ according as $k \equiv |\underline{k}| > |k_0|$, we find

$$\hat{p}(x_2, \underline{k}, \omega)/\rho_0 = \frac{i}{8\pi^2\gamma(k)} \int \hat{Q}(y_2, \underline{K}, \omega) e^{i\{\underline{K} \cdot \underline{y} - \underline{k} \cdot \underline{y} + \gamma(k)|x_2 - y_2|\}} d^3\underline{y} d^2\underline{K}, \quad (2.11)$$

$$|x_2| \rightarrow \infty,$$

where \hat{Q} is defined in terms of Q as in (2.9). Observe that $\hat{Q}(y_2, \underline{K}, \omega)$ is well defined for arbitrary values of y_2 , since $Q(\underline{y}, \tau) \equiv 0$ within the region occupied by the airfoil.

To fix ideas, consider, without loss of generality, the radiation into the region $x_2 > 0$ above the airfoil. The pressure fluctuations in the acoustic far field are determined by the Fourier components $\hat{p}(x_2, \underline{k}, \omega)$ which lie in the acoustic domain $k < |k_0|$. By hypothesis $k_0 a \ll 1$, and it therefore follows that, for turbulence vorticity fluctuations which are confined to the immediate neighborhood of the airfoil, the following approximation may be introduced in the integrand of (2.11):

$$e^{-i\{\underline{k} \cdot \underline{y} + \gamma(k)y_2\}} = e^{-i\underline{k} \cdot \underline{y}} \{1 - i k_1 \phi_1^* - i \gamma(k)y_2\}, \quad (2.12)$$

so that (2.11) may be cast in the form

$$\hat{p}(x_2, \underline{k}, \omega) = \sum_{n=0}^2 \hat{p}_n(x_2, \underline{k}, \omega) \quad (2.13)$$

where

$$\hat{p}_0(x_2, \underline{k}, \omega) / \rho_0 = \frac{i e^{i \gamma(k) x_2}}{2 \gamma(k)} \int \hat{Q}(y_2, \underline{k}, \omega) dy_2, \quad (2.14)$$

$$\hat{p}_1(x_2, \underline{k}, \omega) / \rho_0 = \frac{k_1 e^{i \gamma(k) x_2}}{4 \pi \gamma(k)} \int \hat{Q}(y_2, K_1, k_3, \omega) \phi_1^*(\underline{y}) e^{i(K_1 - k_1) y_1} dy_1 dy_2 dK_1, \quad (2.15)$$

$$\hat{p}_2(x_2, \underline{k}, \omega) / \rho_0 = \frac{e^{i \gamma(k) x_2}}{4 \pi} \int \hat{Q}(y_2, K_1, k_3, \omega) Y_2(\underline{y}) e^{i(K_1 - k_1) y_1} dy_1 dy_2 dK_1. \quad (2.16)$$

The component $\hat{p}_0(x_2, \underline{k}, \omega)$ determines the "quadrupole" radiation generated by the turbulent flow when the influence of the airfoil is ignored, the intensity of which is known to be proportional to $\rho_0 U^3 M^4$. The components \hat{p}_1, \hat{p}_2 represent the sound produced by dipole sources induced on the surface of the airfoil by the unsteady flow and first identified in this context by Curle [10]. The intensity of the dipole sound varies as $\rho_0 U^3 M^3$ and must dominate the radiation field when $M \ll 1$. The contribution from the quadrupoles will be discarded. It will become clear from the ensuing discussion that the radiation fields $p_1(\underline{x}, t)$, $p_2(\underline{x}, t)$ respectively correspond to dipoles whose axes are aligned with the direction of the mean flow and with the x_2 -direction normal to the flow, and that $p_1 = 0$ when the airfoil thickness $s = 0$. They will henceforth be designated the thickness and lift dipoles respectively.

3. THE ACOUSTIC GREEN'S FUNCTION FOR SOURCES NEAR THE TRAILING EDGE

To evaluate the integrals (2.15), (2.16) it is necessary to determine $\phi_1^*(y)$, $y_2(y)$, whose functional forms are dependent on the precise geometrical configuration of the airfoil. Attention is confined to aerodynamic sources $Q(y, \tau)$ near the trailing edge, in the vicinity of which the upper surface of the airfoil is assumed to have the following simple representation:

$$\sigma(x_1) = sx_1/(x_1-d), \quad (x_1 < 0, d \ll 2a), \quad (3.1)$$

so that $\sigma(x_1) \approx s$ far upstream of the edge. As $x_1 \rightarrow 0$,

$$\sigma(x_1) \approx -\epsilon x_1, \quad \epsilon = s/d, \quad (3.2)$$

which implies that the included angle $\bar{\theta} \approx \epsilon$ when $\epsilon \ll 1$.

3.1 Evaluation of $Y_2(\underline{x})$

In the first instance we assume $\epsilon \ll 1$, and introduce the expansion

$$Y_2(\underline{x}) = {}_0Y_2(\underline{x}) + {}_1Y_2(\underline{x}) + \dots, \quad (3.3)$$

where successive terms ${}_nY_2$ are formally of order ϵ^n . Thus ${}_0Y_2$ is the velocity potential of incompressible flow at unit speed in the x_2 -direction when the airfoil is replaced by the flat strip $-2a < x_1 < 0$, $x_2 = 0$, and may be expressed in the form [11, Chapter 6]

$$\left. \begin{aligned} {}_0Y_2(\underline{x}) &= \text{Re}\{-i[(z+a)^2 - a^2]^{1/2}\}, \\ z &= x_1 + ix_2. \end{aligned} \right\} \quad (3.4)$$

In the neighborhood of the trailing edge, where $|z| \sim O(d) \ll a$, this becomes

$${}_0Y_2(\underline{x}) = \text{Re}\{-i(2az)^{1/2}\} . \quad (3.5)$$

The leading order, finite-thickness correction is contained in ${}_1Y_2(\underline{x})$ of (3.3). Near the trailing edge, and to first order in ϵ , the rigid surface condition, $\partial Y_2/\partial x_n = 0$ on the airfoil, may therefore be taken in the form

$$\left. \begin{aligned} \frac{\partial {}_1Y_2}{\partial x_2} &= \frac{\partial}{\partial x_1} \left(\sigma(x_1) \frac{\partial {}_0Y_2}{\partial x_1} \right), & x_1 < 0, x_2 = +0, \\ &= 0, & x_1 < 0, x_2 = -0. \end{aligned} \right\} \quad (3.6)$$

Within the fluid ${}_1Y_2(\underline{x})$ satisfies the two-dimensional Laplace equation

$$\{\partial^2/\partial x_1^2 + \partial^2/\partial x_2^2\} {}_1Y_2 = 0, \quad (3.7)$$

which may be solved by introducing the elementary solution

$$G_0(x_1, x_2; y_1, y_2) = \frac{1}{2\pi} \text{Re}\{\ln(z^{1/2} - z_0^{1/2}) + \ln(z^{1/2} + z_0^{1/2})\}, \quad (3.8)$$

of the problem

$$\{\partial^2/\partial x_1^2 + \partial^2/\partial x_2^2\} G_0 = \delta(x_1 - y_1)\delta(x_2 - y_2), \quad (3.9a)$$

$$\partial G_0/\partial x_2 = 0, \quad x_1 < 0, \quad x_2 = \pm 0, \quad (3.9b)$$

where $z_0 = y_1 + iy_2$, and the asterisk denotes the complex conjugate. Multiply (3.7) by $G_0(x_1, x_2; y_1, y_2)$ and (3.9a) by ${}_1Y_2(\underline{x})$, interchange \underline{x} and \underline{y} , and integrate with respect to y_1, y_2 over the region exterior to the half-plane $y_1 < 0, y_2 = 0$ which is bounded by the circle $\Gamma : (y_1^2 + y_2^2)^{1/2} = R \gg d$. Using Green's theorem [9], this procedure enables ${}_1Y_2$ to be expressed in terms of line integrals over the half-plane and over Γ . It may be assumed that ${}_nY_2(\underline{x})$ does not grow as rapidly as ${}_0Y_1(\underline{x}) \sim O(R^{1/2})$ as $R \rightarrow \infty$. This implies that the representation of ${}_1Y_2(\underline{x})$ does not involve any of the eigenfunctions of the half-plane (which are proportional to $\text{re}\{-iz^{m+1/2}\}$, $m > 0$, and have vanishing normal derivative on $x_1 < 0, x_2 = 0$), and that the contribution from Γ is therefore null. We then find that ${}_1Y_2$ is given by the particular integral

$${}_1Y_2(\underline{x}) = \int_{-\infty}^0 \frac{\partial}{\partial y_1} \left(\sigma(y_1) \frac{\partial {}_0Y_2}{\partial y_1}(y_1, +0) \right) G_0(x_1, x_2; y_1, +0) dy_1 \quad (3.10)$$

This integral is evaluated by making use of (3.1), (3.5), following which one concludes that, near the trailing edge of the airfoil,

$$\begin{aligned} Y_2(\underline{x}) &= {}_0Y_1(\underline{x}) + {}_1Y_2(\underline{x}) \\ &= (2ad)^{1/2} \text{Re}\{w_2(\zeta)\} \end{aligned} \quad (3.11)$$

where,

$$\left. \begin{aligned} w_2(\zeta) &= -i\zeta^{1/2} + \frac{i\epsilon}{4\pi} \frac{\zeta^{1/2} \ln \zeta}{(\zeta-1)} - \frac{\epsilon}{4} \frac{(\zeta^{1/2}-1)}{(\zeta-1)} \\ \zeta &= z/d = (x_1 + ix_2)/d \end{aligned} \right\} \quad (3.12)$$

When ϵ is small this result provides a uniformly valid approximation to $Y_2(\underline{x})$ except possibly in the immediate vicinity of the trailing edge. At such points ($\zeta \sim 0$) it is more appropriate to adopt the renormalized representation:

$$\begin{aligned} w_2(\zeta) &= -i\zeta^{1/2} \{1 + (\epsilon/4\pi)\ln\zeta + i\epsilon/4\} - \epsilon/4 \\ &= -i\zeta^{(1+\epsilon/2\pi)/2} e^{i\epsilon/4} - \epsilon/4 . \end{aligned} \quad (3.13)$$

The adequacy of the above approximations can be assessed by recalling that $Y_2(\underline{x})$ is the velocity potential of a hypothetical flow past the airfoil in the x_2 -direction. It follows that $\text{Im}\{w_2(\zeta)\}$ should be constant on the airfoil. Clearly, (3.12), (3.13) both imply that $\text{Im}\{w_2(\zeta)\} = 0$ on $x_1 < 0$, $x_2 = -0$. Furthermore, from (3.13), $\text{Im}\{w_2(\zeta)\} = 0$ also for $\arg \zeta = \pi - \bar{\theta}$ when $|\zeta| \ll 1$, where

$$\bar{\theta} = \epsilon / (1 + \epsilon/2\pi) , \quad (3.14)$$

i.e., to leading order in ϵ , $\text{Im}\{w_2(\zeta)\} = 0$ on $x_2 = \sigma(x_1)$ in the neighborhood of the sharp trailing edge. For larger values of $|\zeta|$ the actual airfoil profile (3.1) should coincide with that defined by (3.12) in $\text{Im}(\zeta) > 0$. The extent of the agreement for $\epsilon = s/d = \pi/6$ ($\bar{\theta} = 30^\circ$) is illustrated in Figure 3. The solid curve is the profile $\text{Im}\{w_2(\zeta)\} = 0$ computed from the approximation (3.12). The dotted curve depicts the profile (3.1) of the trailing edge of the airfoil.

Actually, it will be argued below that (3.12), (3.13) give a suitable first approximation when ϵ is as large as $2\pi/3$ ($\bar{\theta} = 90^\circ$), when they respectively become "outer" and "inner" representations of $Y_2(\underline{x})$. Of course, the magnitude of the included angle $\bar{\theta}$ must then be taken to be defined by (3.14), and the shape

of the upper surface of the airfoil near the trailing edge is defined by $\text{Im}\{w_2(\zeta)\} = 0$. In all such cases the upper surface has a smooth profile similar to the solid curve in Figure 3, which tends asymptotically to $x_2 = s$ as $x_1 \rightarrow -\infty$.

3.2 Evaluation of $\phi_1^*(\underline{x})$

In this case

$$\left. \begin{aligned} Y_1(\underline{x}) &= x_1 + \phi_1^*(\underline{x}) , \\ \phi_1^*(\underline{x}) &= {}_0\phi_1^*(\underline{x}) + {}_1\phi_1^*(\underline{x}) + \dots \end{aligned} \right\} \quad (3.15)$$

When $\epsilon = 0$ the airfoil degenerates into a plate of zero thickness, and one deduces that ${}_0\phi_1^* \equiv 0$. The leading order effect of finite thickness is contained in ${}_1\phi_1^*(\underline{x})$, whose functional form can be determined by the procedure described above. However, since ${}_0Y_1(\underline{x}) = x_1$, it is necessary to admit the possibility that the representation of ${}_1\phi_1^*(\underline{x})$ includes the eigenfunction $C \cdot \text{Re}(-iz^{1/2})$, $C = \text{constant}$, in addition to a particular integral of the form (3.10) (in which $\partial_0 Y_2 / \partial y_1$ is replaced by $\partial_0 Y_1 / \partial y_1 = 1$). The value of C is chosen to ensure that $Y_1(\underline{x})$ has the correct behavior as $z \rightarrow 0$, i.e., to ensure that $Y_1(\underline{x})$ describes the potential of flow past a wedge of included angle $\bar{\theta}$. In this way one obtains

$$\begin{aligned} Y_1(\underline{x}) &= x_1 + {}_1\phi_1^*(\underline{x}) \\ &= d \text{Re}\{w_1(\zeta)\} , \end{aligned} \quad (3.16)$$

where

$$w_1(\zeta) = \zeta \left\{ 1 - \frac{i\epsilon}{2(\zeta-1)} - \frac{\epsilon \ln \zeta}{2\pi(\zeta-1)} \right\} + \frac{i\epsilon \zeta^{3/2}}{2(\zeta-1)} . \quad (3.17)$$

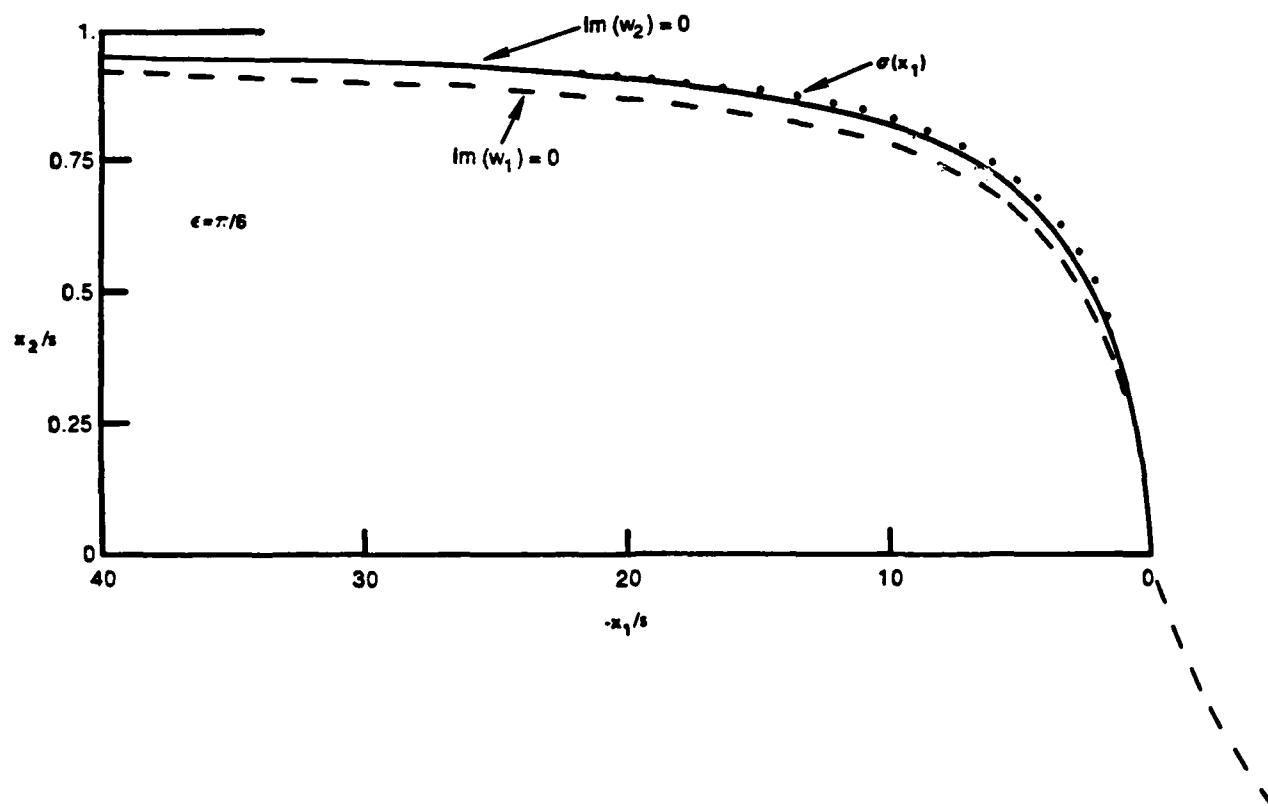


FIGURE 3. PROFILES OF THE UPPER SURFACE OF THE TRAILING EDGE WHEN $\epsilon = \pi/6$: PROFILE DEFINED BY (3.1);
 —: PROFILE DEFINED BY $\text{Im}\{w_2(\zeta)\} = 0$; - - - -:
 PROFILE DEFINED BY $\text{Im}\{w_1(\zeta)\} = 0$.

As $\zeta \rightarrow 0$ this reduces to

$$w_1(\zeta) = \zeta^{(1+\epsilon/2\pi)} e^{i\epsilon/2} . \quad (3.18)$$

The dashed curve in Figure 3 illustrates (for $x_1 < 0$) the profile of the upper surface of the airfoil, as defined by $\text{Im}\{w_1(\zeta)\} = 0$ for $\epsilon = \pi/6$. This tends asymptotically to $x_2 = s$ as $x_1 \rightarrow -\infty$. The differences between this and the actual profile (3.1) are seen to be greater than for the analogous (solid) curve for $Y_2(x)$, although they are not large enough to materially affect the conclusions of the present investigation. The dashed line in the Figure which approaches the edge from $x_1 > 0$, is the dividing streamline of the potential $Y_1(\underline{x})$, and makes an angle $-\bar{\theta}/2$ with the positive x_1 -axis at the stagnation point $x_1 = x_2 = 0$.

As before, when ϵ is not small, equations (3.16), (3.17) will be interpreted as outer and inner approximations to $Y_1(\underline{x})$ for an airfoil whose actual profile is defined by $\text{Im}\{w_1(\zeta)\} = 0$ rather than by (3.1).

4. NOISE PRODUCED BY TURBULENCE ON THE PRESSURE SIDE OF THE AIRFOIL

Consider first the sound produced by boundary layer turbulence convecting past the trailing edge in the region $x_2 < 0$ below the airfoil. The integrations with respect to y_1 in (2.15), (2.16) may then be assumed to extend over the interval $(-\infty, \infty)$ without encountering the airfoil.

4.1 The Lift Dipole $p_2(\underline{x}, t)$

Using (3.11) in (2.16) we have

$$\hat{p}_2(x_2, \underline{k}, \omega)/\rho_0 = \frac{(2ad)^{1/2} e^{i\gamma(k)x_2}}{4\pi} \int \hat{Q}(y_2, K_1, k_3, \omega) \text{Re}\{w_2(\zeta_0)\} \times e^{i(K_1 - k_1)y_1} dy_1 dy_2 dK_1, \quad (4.1)$$

where $\zeta_0 = (y_1 + iy_2)/d$. To evaluate the y_1 -integral, we set

$$\begin{aligned} I(\alpha) &= \int_{-\infty}^{\infty} \text{Re}\{w_2(\zeta_0)\} e^{i\alpha y_1} dy_1 \\ &= \frac{1}{2} \{I'(\alpha) + \text{c.c.} I'(-\alpha)\}, \quad \alpha = K_1 - k_1, \end{aligned} \quad (4.2)$$

where,

$$I'(\alpha) = \int_{-\infty}^{\infty} w_2(\zeta_0) e^{i\alpha y_1} dy_1, \quad (4.3)$$

and "c.c." denotes "complex conjugate." $I'(\alpha)$ can be written as the following function theoretic contour integral:

$$I'(\alpha) = d e^{\alpha y_2} \int_{-iy_2/d}^{+iy_2/d} w_2(\zeta_0) e^{i\alpha d \zeta_0} d\zeta_0, \quad (4.4)$$

the path of integration in the ζ_0 -plane being parallel to the real axis at distance y_2/d (<0).

According to equation (3.12) the integral (4.4) is formally divergent. Since, however, the aerodynamic source $Q(y, \tau)$ may be assumed to vanish as $y_1 \rightarrow \pm\infty$, the value of the divergent integral may be interpreted as a generalized function, as in classical thin airfoil theory [12]. To do this the integral is expressed as the derivative with respect to α of a convergent integral, as follows:

$$I'(\alpha) = -ie^{\alpha y_2} \frac{\partial}{\partial \alpha} \int_{-iy_2/d}^{+iy_2/d} \frac{w_2(\zeta_0) e^{i\alpha d \zeta_0} d\zeta_0}{\zeta_0}. \quad (4.5)$$

The integrand is regular in the ζ_0 -plane, except for the branch point at $\zeta_0 = 0$, and $w_2(\zeta_0)/\zeta_0 \rightarrow 0$ as $|\zeta_0| \rightarrow \infty$. Thus $I'(\alpha) \equiv 0$ for $\alpha < 0$ (and $y_2 < 0$). For $\alpha > 0$ the integration contour may be deformed onto a branch-cut extending from the origin to $+i\infty$, and $I'(\alpha)$ can then be re-expressed in the form

$$I'(\alpha) = \frac{d(i\pi)^{1/2} e^{\alpha y_2} F_2(\alpha d)}{(\alpha d)^{3/2}} \quad \alpha > 0, \quad \left. \vphantom{\frac{d(i\pi)^{1/2} e^{\alpha y_2} F_2(\alpha d)}{(\alpha d)^{3/2}}} \right\} \quad (4.6)$$

$$F_2(x) = 1 - \epsilon x f(x),$$

where

$$f(x) = \frac{1}{4\pi^{1/2}} \left\{ \left(1 + \frac{2i \ln x}{\pi} \right) \int_0^\infty \frac{u^{1/2} e^{-u}}{u+ix} du - \frac{2i}{\pi} \int_0^\infty \frac{u^{1/2} \ln u e^{-u}}{u+ix} du \right\} \quad (4.7)$$

which is readily evaluated numerically (or in terms of tabulated functions for the first of the integrals on the right hand side;

see [13]). When $I'(-\alpha)$ is evaluated in the same way, we find from (4.2)

$$I(\alpha) = \frac{d(i\pi)^{1/2} e^{|\alpha|y_2}}{2(\alpha d)^{3/2}} \operatorname{sgn}(\alpha) F_2(\alpha d) . \quad (4.8)$$

In obtaining this result use has been made of the "outer" representation (3.12) of $w_2(\zeta)$. It is evident from the discussion of Section 3 that this is likely to be an adequate approximation only if the principal contributions to the branch-cut integrals in (4.7) are not from the neighborhood of the branch point $\mu = 0$, where the functional form of $w_2(\zeta)$ is determined by the geometry of airfoil at the sharp trailing edge. Thus (4.6) must cease to be valid when $x \equiv \alpha d \rightarrow \infty$, in which case $xf(x)$ becomes logarithmically large. In that limit (4.6) implies that, provided $\epsilon \rightarrow 0$,

$$F_2(x) = 1 + \frac{i\epsilon}{8} \left(1 + \frac{2i \ln x}{\pi} \right) + \frac{\epsilon}{4\pi} \left(2 - \gamma_e - \ln 4 \right) , \quad (4.9)$$

where $\gamma_e = 0.577216\dots$, is Euler's constant ([13], page 255).

Now the correct behavior of $F_2(x)$ as $x \rightarrow \infty$, which takes proper account of the behavior of $w_2(\zeta)$ at the sharp edge of the airfoil, must be given by use of the asymptotic, "inner" approximation (3.13) in the integrand of (4.5), which yields

$$F_2(x) = (2/\pi)^{1/2} (1+i\epsilon/8) \Gamma(3/2+\epsilon/4\pi) x^{-\epsilon/4\pi} , \quad (4.10)$$

in terms of the gamma function $\Gamma(z)$ [13]. This reduces to (4.9) when expanded to first order in ϵ , and use is made of formulae given in Section 6.3.4 of reference [13]. For small values of ϵ , (4.9), (4.10) are both well approximated in their respective regions of validity by

$$F_2(x) = \exp \left\{ \frac{i\epsilon}{8} \left(1 + \frac{2i \ln x}{\pi} \right) + \frac{\epsilon}{4\pi} \left(2 - \gamma_e - \ln 4 \right) \right\} . \quad (4.11)$$

It follows that a uniformly valid approximation, which gives the correct behavior of $F_2(x)$ for small and large values of x is obtained by replacing $1-\epsilon x f(x)$ in (4.6) by $\exp\{-\epsilon x f(x)\}$. With this renormalization, equation (4.8) becomes

$$I(\alpha) = \frac{d(\pi i)^{1/2} Z_2(\alpha d) e^{|\alpha| y_2}}{2(\alpha d)^{3/2}}, \quad (4.12)$$

where

$$Z_2(x) = \text{sgn}(x) F_2(x) = \text{sgn}(x) \exp\{-\epsilon x f(x)\}, \quad (4.13)$$

so that $Z_2(x) \approx x^{-\epsilon/4\pi}$ as $x \rightarrow \infty$. This is actually expected to be a good approximation for $\epsilon \lesssim 2\pi/3$ ($\bar{\theta} \lesssim 90^\circ$). Indeed, the exponent in (4.13) is then small except when x is large, and in that case the asymptotic result (4.10) is still well approximated by (4.11) for such values of ϵ , since $\Gamma(z)$ is stationary in the neighborhood of $z = 3/2$.

Using this representation for $I(\alpha)$ in (4.1), and taking the inverse Fourier transform, we obtain for the lift-dipole component of the acoustic pressure

$$p_2(\underline{x}, t)/\rho_0 = \frac{(ai/2\pi)^{1/2}}{4} \int \frac{\hat{Q}(y_2, K_1, k_3, \omega) Z_2\{(K_1 - k_1)d\}}{(K_1 - k_1)^{3/2}} \\ \times \exp[i[k \cdot \underline{x} + \gamma(k)x_2 - \omega t] + |K_1 - k_1| y_2] d^2 \underline{k} d\omega dK_1 dy_2, \\ x_2 \rightarrow +\infty, \quad y_2 < 0. \quad (4.14)$$

When $\epsilon = 0$, $Z_2(x) = \text{sgn}(x)$, and this expression reduces to that for a flat-plate airfoil of chord $2a$.

It has already been noted (in Section 2) that, in the acoustic far field, the dominant contribution to the integral with respect to \underline{k} in (4.14) is from the acoustic region $k < |k_0|$, whereas, as will be seen below, the important values of K_1 in the integrand are associated with the hydrodynamic region $K_1 \sim \omega/U \gg k_0$ of the boundary layer wall pressure fluctuations. Accordingly (4.14) may be further simplified to the form

$$p_2(\underline{x}, t)/\rho_0 = \frac{(ai/2\pi)^{1/2}}{4} \int \frac{\hat{Q}(y_2, K_1, k_3, \omega) Z_2\{K_1 d\}}{K_1^{3/2}} \\ \times \exp\{i[\underline{k} \cdot \underline{x} + \gamma(k)x_2 - \omega t] + |K_1|y_2\} d^2 \underline{k} d\omega dK_1 dy_2, \\ x_2 \rightarrow +\infty, y_2 < 0. \quad (4.14)$$

4.2 The Thickness Dipole $p_1(\underline{x}, t)$

A similar analysis can be given for the simplification of the integral representation (2.15) of $p_1(x_2, \underline{k}, \omega)$ by making use of the formulae (3.17), (3.18) for $w_1(\zeta)$. In this case one finds

$$p_1(\underline{x}, t)/\rho_0 = \frac{\epsilon(id/\pi)^{1/2}}{8} \int \frac{k_1 \hat{Q}(y_2, K_1, k_3, \omega) Z_1(K_1 d)}{\gamma(k) K_1^{3/2}} \\ \times \exp\{i[\underline{k} \cdot \underline{x} + \gamma(k)x_2 - \omega t] + |K_1|y_2\} d^2 \underline{k} d\omega dK_1 dy_2, \\ x_2 \rightarrow +\infty, y_2 < 0, \quad (4.15)$$

where

$$Z_1(x) = -\text{sgn}(x) \left\{ 1 - \frac{2ix}{\pi^{1/2}} \int_0^\infty \frac{\mu^{1/2} e^{-\mu}}{\mu + ix} d\mu \right. \\ \left. - (x/\pi i)^{1/2} \int_0^\infty \frac{\mu e^{-\mu}}{\mu + ix} d\mu \right\} \quad (4.16)$$

and $Z_1(x) = x^{-1/2}$ as $x \rightarrow \infty$.

5. THE KUTTA CONDITION

The aeroacoustic source term $Q(\underline{x}, t)$ on the right of equation (2.2) consists of two distinct and identifiable components. The first involves vorticity ω in the boundary layer which is convected into the trailing edge region from upstream. The second is associated with vorticity which is generated at the surface of the airfoil in the vicinity of the edge (and subsequently shed into the wake) in response to the unsteady forcing by the incident boundary layer disturbances. In this section the properties of the shed vorticity will be estimated on the basis of high Reynolds number, unsteady airfoil theory, i.e., the Kutta condition will be imposed, which requires that the motion induced by the shed vorticity at the trailing edge is such as to remove the singularities in pressure and velocity that would otherwise be predicted to occur there in ideal, inviscid flow. This procedure is believed to be valid provided the reduced frequency $\omega s/U$ is not too large [14].

5.1 The Green's Function $G(\underline{x}, \underline{y}, t, \tau)$ for \underline{x} Near the Trailing Edge

Consider first the motion induced near the trailing edge by a single Fourier component $\hat{q}(x_2, K_1, k_3, \omega) e^{i(\underline{K} \cdot \underline{x} - \omega t)}$, say, of the boundary layer disturbances in $x_2 < 0$ which are incident on the edge from upstream. When the ultimate objective is the determination of the acoustic radiation by use of the dipole formulae (4.14), (4.15), attention may be confined to wavenumbers $\underline{K} = (K_1, 0, k_3)$, where k_3 lies in the acoustic domain $|k_3| < |k_0|$. In that case the flow produced near the edge by this source is essentially two-dimensional, inasmuch as the length scale of variation in the spanwise direction is large relative to all other scales of the flow. In order to calculate the velocity near the edge from the integral representation (2.5) of the stagnation enthalpy, it is evidently sufficient to determine the functional form of the Green's function from the reduced equation

$$\{\partial^2/\partial x_1^2 + \partial^2/\partial x_2^2\}G = -\delta(\underline{x}-\underline{y})\delta(t-\tau), \quad (5.1)$$

wherein $\partial^2 G/c^2 \partial t^2$ is neglected because retarded time effects are negligible in the vicinity of the edge, i.e., the flow may be taken to be locally incompressible and two-dimensional.

To solve (5.1), set

$$G(\underline{x}, \underline{y}, t, \tau) = -\{G_0(x_1, x_2; y_1, y_2) + G_1(x_1, x_2; y_1, y_2) + \dots\} \delta(x_3 - y_3) \delta(t - \tau), \quad (5.2)$$

where G_0 is the potential of incompressible flow produced by the line source $\delta(x_1 - y_1)\delta(x_2 - y_2)$ in the presence of the rigid half-plane $x_1 < 0$, $x_2 = 0$ (as defined by (3.8)), and G_1 is an $O(\epsilon)$ correction which accounts for the leading order effects of finite thickness of the airfoil. G_1 satisfies the homogeneous Laplace equation and is subject to a boundary condition of the form (3.6), namely

$$\left. \begin{aligned} \frac{\partial G_1}{\partial x_2} &= \frac{\partial}{\partial x_1} \left\{ \sigma(x_1) \frac{\partial G_0}{\partial x_1} \right\}, & x_1 < 0, x_2 = +0, \\ &= 0, & x_1 < 0, x_2 = -0. \end{aligned} \right\} \quad (5.3)$$

It follows by the method of Section 3, equation (3.10), that

$$\begin{aligned} &G_1(x_1, x_2; y_1, y_2) \\ &= \text{Re} \left\{ \frac{i\epsilon}{8\pi^2} \int_0^\infty \left[\frac{1}{[\lambda^{1/2} + i\zeta_0^{1/2}]} + \frac{1}{[\lambda^{1/2} - i\zeta_0^{1/2}]} \right] \frac{d\lambda}{(\lambda+1)(\zeta^{1/2} - i\lambda^{1/2})} \right\}, \end{aligned} \quad (5.4)$$

where $\zeta = (x_1 + ix_2)/d$, $\zeta_0 = (y_1 + iy_2)/d$. This integral is readily evaluated for arbitrary values of ζ , but to apply the Kutta condition only the behavior near the trailing edge $\zeta = 0$ is required. Expanding (5.4) for small values of ζ , and combining the result with the corresponding expansion of G_0 , one finds for $\zeta/\zeta_0 \ll 1$,

$$G(\underline{x}, \underline{y}, t, \tau) = \frac{1}{2\pi} \delta(x_3 - y_3) \delta(t - \tau) \\ \times \operatorname{Re} \left\{ \zeta^{1/2} \left[\frac{1}{\zeta_0^{1/2}} \left(1 - \frac{i\epsilon(\zeta_0^{1/2} - 1)}{4(\zeta_0 - 1)} + \frac{\epsilon}{4\pi} \left\{ \ln \zeta + \frac{\ln \zeta_0}{(\zeta_0 - 1)} \right\} + \frac{i\epsilon}{4} \right) \right. \right. \\ \left. \left. - \frac{1}{\zeta_0^{*1/2}} \left(1 + \frac{i\epsilon(\zeta_0^{*1/2} - 1)}{4(\zeta_0^* - 1)} + \frac{\epsilon}{4\pi} \left\{ \ln \zeta + \frac{\ln \zeta_0^*}{(\zeta_0^* - 1)} \right\} + \frac{i\epsilon}{4} \right) \right] \right\}. \quad (5.5)$$

This "outer" approximation can be renormalized (as in Section 3) in the limit as $\zeta \rightarrow 0$, yielding

$$G(\underline{x}, \underline{y}, t, \tau) = \frac{1}{\pi} (x_3 - y_3) \delta(t - \tau) \\ \times |x_1^2 + x_2^2|^{(1+\epsilon/2\pi)/4} \sin \left\{ \frac{\xi}{2} \left(1 + \frac{\epsilon}{2\pi} \right) + \frac{\epsilon}{4} \right\} \operatorname{Re} \{ w_g(\zeta_0) \}, \quad (5.6)$$

where,

$$w_g(\zeta_0) = \frac{i}{\zeta_0^{1/2}} \left\{ 1 - \frac{i\epsilon(\zeta_0^{1/2} - 1)}{4(\zeta_0 - 1)} + \frac{\epsilon \ln \zeta_0}{4\pi(\zeta_0 - 1)} \right\}, \quad \left. \vphantom{\frac{i}{\zeta_0^{1/2}}} \right\} \quad (5.7)$$

$$\xi = \arg(\zeta).$$

Observe that $\partial G / \partial \xi = 0$ for $\xi = -\pi, \pi(1 - \epsilon/2\pi)/(1 + \epsilon/2\pi)$, i.e., on the faces of the wedge shaped tip of the airfoil, as required.

5.2 Induced Flow Near the Edge

Inserting (5.6) into (2.5), with $Q(y, \tau)$ replaced by

$$\hat{q}(y_2, K_2, k_3, \omega) e^{i(K \cdot Y - \omega \tau)},$$

integrating over all values of K_1 , and denoting by B_q the corresponding unsteady stagnation enthalpy, we find that near the edge

$$B_q = \frac{1}{\pi} |x_1^2 + x_2^2|^{(1+\epsilon/2\pi)/4} \sin\left\{\frac{\epsilon}{2}\left(1 + \frac{\epsilon}{2\pi}\right) + \frac{\epsilon}{4}\right\} e^{i(k_3 x_3 - \omega t)} \\ \times \int \hat{q}(y_2, K_1, k_3, \omega) \operatorname{Re}\{w_g(\zeta_0)\} e^{iK_1 y_1} dy_1 dy_2 dK_1. \quad (5.8)$$

As previously, the integration with respect to y_1 can be simplified by transformation into a contour integral in the ζ_0 -plane, leading to

$$B_q = \frac{d}{\pi} |x_1^2 + x_2^2|^{(1+\epsilon/2\pi)/4} \sin\left\{\frac{\epsilon}{2}\left(1 + \frac{\epsilon}{2\pi}\right) + \frac{\epsilon}{4}\right\} e^{i(k_3 x_3 - \omega t)} \\ \times \int \mathcal{F}(K_1 d) \hat{q}(y_2, K_1, k_3, \omega) e^{|K_1| y_2} dy_2 dK_1, \quad (y_2 < 0), \quad (5.9)$$

where,

$$\mathcal{F}(x) = -\operatorname{sgn}(x) \{\pi/ix\}^{1/2} \left\{ 1 - \frac{i\epsilon}{8} \left[1 + \frac{2i}{\pi} [\ln x + \gamma_e + \ln 4] \right] + \frac{i\epsilon}{2} f(x) \right\}, \quad (5.10)$$

and $f(x)$ is defined as in (4.7).

For fixed ϵ , the term in the brace brackets of (5.10) becomes unbounded as $x \equiv K_1 d + \infty$. This occurs because the integral with respect to y_1 is then dominated by the behavior of $w_g(\zeta_0)$ near the sharp edge $\zeta_0 = 0$ of the airfoil. The correct behavior is obtained by use of an "inner" representation of $w_g(\zeta_0)$ as a function of ζ_0 . By this means one finds, by the procedure justified in Section 3, that the following exponential renormalization of $\mathfrak{F}(x)$ is valid for all values of x

$$\mathfrak{F}(x) = \frac{-(\pi/i)^{1/2} \operatorname{sgn}(x)}{x^{(1-\epsilon/2\pi)/2}} \cdot \exp\left\{\frac{\epsilon}{4\pi}(\gamma_e + \ln 4) + \frac{i\epsilon}{2}[f(x) - 1/4]\right\} \quad (5.11)$$

Equations (5.9), (5.11) determine the fluid motion near the sharp trailing edge of the airfoil. Vorticity in $x_2 < 0$ produces a disturbance $B_g = -\partial\phi_g/\partial t$, say, in $x_2 > 0$, where ϕ_g is a velocity potential. It follows from (5.9) that the corresponding velocity becomes singular like $|x_1^2 + x_2^2|^{-(1-\epsilon/2\pi)/4}$ at the edge.

5.3 The Shed Vorticity

According to the unsteady Kutta condition sufficient vorticity is in practice shed from the edge to remove this singular behavior. It will be assumed that the shed vorticity convects downstream in the plane $x_2 = 0$ at velocity U_g , say. Let $\hat{q}_g(x_2, \underline{K}, \omega)$, $\underline{K} = (K_1, 0, k_3)$, denote the Fourier transform of the equivalent hydroacoustic source due to the shed vorticity, so that, by the second of equations (2.2), we can write

$$\hat{q}_g(x_2, \underline{K}, \omega) = \frac{\partial}{\partial x_2} \{N(k_3, \omega) \delta(x_2) \delta(K_1 - \omega/U_g)\} \quad (5.12)$$

where $N(k_3, \omega)$ is to be determined.

Observe that, since $\partial G/\partial y_2 = 0$ (i.e., $\operatorname{Re}\{\partial w_g/\partial y_2\} = 0$) on the pressure side $y_1 < 0$, $y_2 = -0$ of the airfoil, the integral (2.5) which defines the stagnation enthalpy field B_g , say, produced by

the shed vorticity, may be assumed to extend over the range $-\infty < y_1 < +\infty$. It follows that the behavior of B_s near the edge is given by an integral of the form (5.9) for each k_3, ω , and, therefore, that the Kutta condition will be fulfilled provided

$$\int \{ \hat{q}(y_2, K_1, k_3, \omega) + \hat{q}_s(y_2, K_1, k_3, \omega) \} \mathcal{F}(K_1 d) e^{|K_1| y_2} dy_2 dK_1 = 0. \quad (5.13)$$

On introducing (5.12), this implies that

$$N(k_3, \omega) = \frac{1}{|\omega/U_s| \mathcal{F}(\omega d/U_s)} \int \hat{q}(y_2, K_1, k_3, \omega) \mathcal{F}(K_1 d) e^{|K_1| y_2} dy_2 dK_1. \quad (5.14)$$

Hence, in using (4.14), (4.15) to calculate the lift and thickness dipole radiation fields produced by turbulent flow past the trailing edge on the pressure side of the airfoil, one must take

$$\hat{Q}(x_2, K_1, k_3, \omega) = \hat{q}(x_2, K_1, k_3, \omega) +$$

$$\frac{\partial}{\partial x_2} \left\{ \frac{\delta(x_2) \delta(K_1 - \omega/U_s)}{|K_1| \mathcal{F}(K_1 d)} \int \hat{q}(y_2', \kappa, k_3, \omega) \mathcal{F}(\kappa d) e^{|\kappa| y_2'} dy_2' d\kappa \right\}, \quad (5.15)$$

where $\hat{q}(x_2, K, \omega)$ is the Fourier transform of the hydroacoustic sources in the boundary layer (defined as in (2.2)) which are convected into the trailing edge region from upstream, and the second term on the right hand side accounts for the influence of the shed vorticity.

6. THE RADIATED SOUND

6.1 The Acoustic Pressure Spectra

Using the representation (5.15) in equation (4.14) for the lift dipole, we obtain

$$p_2(\underline{x}, t) / \rho_0 = \frac{(ai/2\pi)^{1/2}}{4} \int \frac{\hat{q}(y_2, K_1, k_3, \omega) Z_2\{K_1 d\}}{K_1^{3/2}} \\ \times \left\{ 1 - \left(\frac{K_1}{\omega/U_s} \right)^{3/2} \frac{Z_2(\omega d/U_s) \mathcal{F}(K_1 d)}{Z_2(K_1 d) \mathcal{F}(\omega d/U_s)} \right\} \\ \times \exp\{i[\underline{k} \cdot \underline{x} + \gamma(k)x_2 - \omega t] + |K_1|y_2\} d^2 \underline{k} d\omega dK_1 dy_2, \\ x_2 \rightarrow +\infty, y_2 < 0, \quad (6.1)$$

where the second term in the brace brackets of the integrand corresponds to the sound produced by the shed vorticity, and should be omitted when the Kutta condition is not applied.

The frequency spectrum $\phi_2(\omega)$, say, of the acoustic pressure associated with turbulent boundary layer flow of finite spanwise extent l (which may be assumed to straddle the origin of coordinates, as in Figure 4) may now be determined. At the far field point \underline{x} , $\phi_2(\omega)$ satisfies

$$\langle p_2^2(\underline{x}, t) \rangle = \int_{-\infty}^{\infty} \phi_2(\omega) d\omega,$$

where the angle brackets $\langle \rangle$ denote an ensemble average. It will be assumed that the density $q(\underline{x}, t)$ of the hydroacoustic sources in $x_2 < 0$ which are convected into the trailing edge region from upstream is a stationary random function of x_1, x_3 , and t , such that

$$\langle \hat{q}(x_2, \underline{K}, \omega) \hat{q}^*(x_2', \underline{K}', \omega') \rangle = S(x_2, x_2'; \underline{K}, \omega) \delta(\underline{K} - \underline{K}') \delta(\omega - \omega'), \quad (6.3)$$

where $S(x_2, x_2'; K, \omega)$ is the cross-spectral density of the hydro-acoustic sources [15]. This hypothesis is consistent with the assumption that the boundary layer sources are convected past the trailing edge in an essentially frozen configuration. The integration in (6.1) with respect to k_1, k_3 may be evaluated asymptotically as $|\underline{x}| \rightarrow \infty$ (e.g., by the method of stationary phase), following which one finds

$$\begin{aligned} \Phi_2(\omega) = & \frac{ak_0^2 \cos^2 \theta}{16|\underline{x}|^2} \int S(y_2, y_2'; K_1, k_0 \sin \theta \sin \phi, \omega) \exp\{|K_1|(y_2 + y_2')\} \\ & \times \left| 1 - \left(\frac{K_1}{\omega/U_s}\right)^{3/2} \frac{Z_2(\omega d/U_s) \mathcal{F}(K_1 d)}{Z_2(K_1 d) \mathcal{F}(\omega d/U_s)} \right|^2 \frac{|Z_2(K_1 d)|^2}{|K_1|^3} dK_1 dy_2 dy_2' , \end{aligned} \quad (6.4)$$

where $(|\underline{x}|, \theta, \phi)$ are the spherical polar coordinates of the far field observer position \underline{x} illustrated in Figure 4. The linear dependence of this result on $\cos^2 \theta$ is characteristic of the radiation field of a dipole orientated in the x_2 -direction.

A similar calculation starting from equation (4.15) for the thickness dipole yields the following expression for the corresponding frequency spectrum $\Phi_1(\omega)$:

$$\begin{aligned} \Phi_1(\omega) = & \frac{1d\epsilon^2 \cos^2 \psi}{32|\underline{x}|^2} \int S(y_2, y_2'; K_1, k_0 \sin \theta \sin \phi, \omega) \exp\{|K_1|(y_2 + y_2')\} \\ & \times \left| 1 - \left(\frac{K_1}{\omega/U_s}\right)^{3/2} \frac{Z_1(\omega d/U_s) \mathcal{F}(K_1 d)}{Z_1(K_1 d) \mathcal{F}(\omega d/U_s)} \right|^2 \frac{|Z_1(K_1 d)|^2}{|K_1|^3} dK_1 dy_2 dy_2' , \end{aligned} \quad (6.5)$$

where ψ is the angle between the observer direction \underline{x} and the positive x_1 -axis.

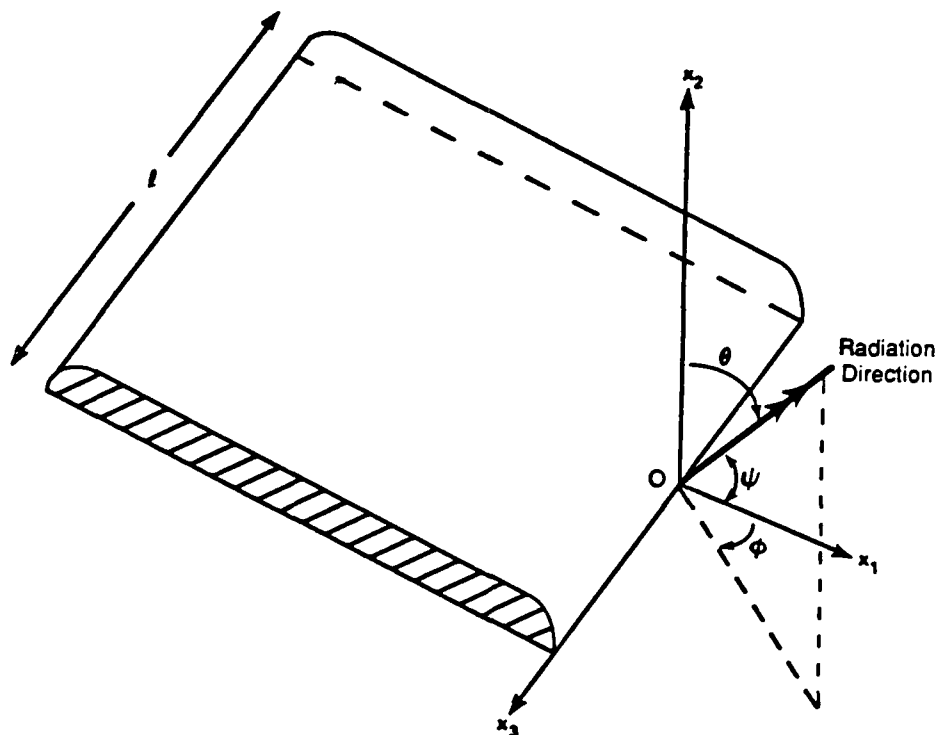


FIGURE 4. COORDINATES DEFINING THE RADIATION INTO THE FAR FIELD.

Note that, the radiation fields $p_1(\underline{x}, t)$, $p_2(\underline{x}, t)$ are not statistically independent, and the spectrum of the net field $p_1 + p_2$ is not, therefore, equal to $\phi_1(\omega) + \phi_2(\omega)$. However, it will be seen below that the thickness dipole is generally negligible except possibly at $\theta = \pi/2$, i.e., in planes parallel to the mean flow, where ϕ_2 is null.

6.2 The Boundary Layer Turbulence

At distances far upstream of the trailing edge of the airfoil, the surface pressure fluctuations can be expressed simply in terms of the hydroacoustic source density $q(\underline{x}, t)$. If $P_O(\underline{K}, \omega)$ denotes the wavenumber-frequency spectrum of the surface pressures [16], then for the plane surface $x_2 = -0$, $P_O(\underline{K}, \omega)$ and $S(x_2, x_2'; \underline{K}, \omega)$ are found to be related by

$$P_O(\underline{K}, \omega) = \frac{\rho_O^2 (1 - U_O K_1 / \omega)^2}{|\gamma(\underline{K})|^2} \int_{-\infty}^0 S(y_2, y_2'; \underline{K}, \omega) \times \exp\{-i[\gamma(\underline{K})y_2 - \gamma^*(\underline{K})y_2']\} dy_2 dy_2' , \quad (6.6)$$

where U_O is the mean flow speed (in the x_1 -direction) just outside the viscous sublayer (see, e.g., [4]). In this result the cross-spectrum $S(y_2, y_2'; \underline{K}, \omega)$ may be identified with that appearing in the representations (6.4), (6.5) of the acoustic spectra provided the boundary layer turbulence convects past the trailing in an essentially frozen pattern. This will be assumed to be the case.

Now it is known [16] that $P_O(\underline{K}, \omega)$ is sharply peaked in the neighborhood of the "convective ridge" centered on $K_1 = \omega/U_C$, $K_3 = 0$, where U_C is a convection velocity which is typically equal to 70% of the main stream velocity U , and varies slowly with frequency. In these circumstances (6.6) implies that

$$\begin{aligned} \int_{-\infty}^0 \int_{-\infty}^0 S(y_2, y_2'; K_1, k_O \sin \theta \sin \phi, \omega) e^{iK_1(y_2 + y_2')} dy_2 dy_2' \\ = \frac{|K_1|^2 P_O(K_1, k_O \sin \theta \sin \phi, \omega)}{\rho_O^2 (1 - U_O K_1 / \omega)^2} = \frac{|K_1|^2 P_O(K_1, 0, \omega)}{\rho_O^2 (1 - U_O K_1 / \omega)^2} , \quad (6.7) \end{aligned}$$

and equation (6.4) for $\phi_2(\omega)$ becomes:

$$\phi_2(\omega) = \frac{ak_0^2 \cos^2 \theta}{16|\underline{x}|^2} \int_{-\infty}^{\infty} \frac{P_0(K_1, 0, \omega)}{(1 - U_0 K_1 / \omega)^2} \times \left| 1 - \left(\frac{K_1}{\omega/U_s} \right)^{3/2} \frac{Z_2(\omega d/U_s) \mathcal{F}(K_1 d)}{Z_2(K_1 d) \mathcal{F}(\omega d/U_s)} \right|^2 \frac{|Z_2(K_1 d)|^2}{|K_1|} dK_1 \quad (6.8)$$

Z_2 and \mathcal{F} are slowly varying functions of their arguments, so that the value of this integral may be approximated by setting $K_1 = \omega/U_c$ in all terms of the integrand except $P_0(K_1, 0, \omega)/|K_1|$, leading to

$$\phi_2(\omega) = \frac{ak_0^2 \cos^2 \theta}{16|\underline{x}|^2} \left| \exp\{-2\epsilon(\omega d/U_c) f(\omega d/U_c)\} \right| \times \left| \frac{1 - (U_s/U_c)^{(1+\epsilon/4\pi)} \exp\{\epsilon[\omega d/U_c + i/2]f(\omega d/U_c) - \epsilon[\omega d/U_s + i/2]f(\omega d/U_s)\}}{(1 - U_0/U_c)} \right|^2 \times \int_{-\infty}^{\infty} \frac{P_0(K_1, 0, \omega)}{|K_1|} dK_1 \quad (6.9)$$

where use has been made of (4.7), (4.13), and (5.11).

The value of the remaining integral in this result may be estimated by making use of Chase's [16] empirical formula for $P_0(K, \omega)$, which is valid in the vicinity of the convective domain:

$$P_0(K_1, 0, \omega) = \frac{C_m \rho^2 v_*^3 K_1^2}{[(\omega - U_c K_1)^2 / (h v_*)^2 + K_1^2 + (b\delta)^{-2}]^{5/2}} \quad (6.10)$$

where v_* is the friction velocity, δ the boundary layer thickness, and the remaining parameters are given by

$$b = 0.75, \quad C_m = 0.1553, \quad h = 3. \quad (6.11)$$

Using this in (6.9), we finally obtain

$$\begin{aligned} \frac{c^2 \phi_2(\omega)}{\rho_o^2 v_*^4 U \delta (al/|x|^2)} &= \frac{(C_m h/12)(U_c/U) \cos^2 \theta [1 + (hv_*/U_c)^2]^{1/2} (\omega \delta/U_c)^3}{[(\omega \delta/U_c)^2 + (1 + (hv_*/U_c)^2)/b^2]^2} \\ &\times |\exp\{-2\epsilon(\omega \delta/U_c) f(\omega \delta/U_c)\}| \\ &\times \left| \frac{1 - (U_s/U_c)^{(1+\epsilon/4\pi)} \exp\{\epsilon[\omega \delta/U_c + i/2] f(\omega \delta/U_c) - \epsilon[\omega \delta/U_s + i/2] f(\omega \delta/U_s)\}}{(1 - U_o/U_c)} \right|^2. \end{aligned} \quad (6.12)$$

When $\epsilon = 0$ this result reduces to the spectrum of the lift dipole when the airfoil has zero thickness.

An analogous calculation leads to the following explicit representation of the spectrum (6.5) of the thickness dipole:

$$\begin{aligned} \frac{c^2 \phi_1(\omega)}{\rho_o^2 v_*^4 U \delta (al/|x|^2)} &= \frac{\epsilon^3 (C_m h/24)(s/a)(U_c/U) \cos^2 \psi [1 + (hv_*/U_c)^2]^{1/2} (\omega \delta/U_c)^3}{[(\omega \delta/U_c)^2 + (1 + (hv_*/U_c)^2)/b^2]^2} \\ &\times \frac{|Z_1(\omega \delta/U_c)|^2}{(1 - U_o/U_c)^2} \left| 1 - (U_s/U_c)^{1+\epsilon/4\pi} \cdot \frac{\exp\{(i\epsilon/2)[f(\omega \delta/U_c) - f(\omega \delta/U_s)]\}}{\{Z_1(\omega \delta/U_c)/Z_1(\omega \delta/U_s)\}} \right|^2, \end{aligned} \quad (6.13)$$

In applying these formulae the value of ϵ is determined in terms of the included $\bar{\theta}$ of the trailing edge by the following form of (3.14):

$$\epsilon = \bar{\theta}/(1-\bar{\theta}/2\pi) \quad (6.14)$$

6.3 Numerical Results

These formulae will now be used to illustrate the predicted influence of trailing edge beveling on the radiated sound. Consider first the acoustic pressure spectrum of the lift dipole, given by (6.12). It is necessary to specify the convection velocities U_0 , U_s , U_c . In applications it is often the relatively high frequency range $\omega\delta/U \gg 1$ that is of interest. In a first approximation the shed vorticity might then be expected to convect downstream at a velocity equal to the mean velocity in the boundary layer just outside the viscous sublayer ($\approx 0.7v_*$), where vorticity generation occurs. This hypothesis will be adopted in the absence of reliable experimental data to the contrary. Since, typically, $v_* \approx 0.04U$, we shall take $U_s = U_0 = 7v_* \approx 0.25U$ (see [17], page 629). The convection velocity of disturbances in the main body of the boundary layer will be taken to be given by $U_c = 0.7U$.

With these qualifications, the predicted variations of the lift dipole spectrum $10.\log_{10}\{c^2\phi_2(\omega)/\rho_0^2v_*^4U\delta(a\ell|x|^2)\cos^2\theta\}$ (dB) with frequency $\omega\delta/U$, for turbulence on the pressure side of the airfoil, are depicted in Figures 5(a), (b) respectively for $\delta/s = 0.1, 1$. The different curves in these figures are for trailing edges of included angles $\bar{\theta} = 0^\circ, 30^\circ, 60^\circ$, and 90° . When $\bar{\theta} = 0$ the airfoil is flat. Increasing the value of $\bar{\theta}$ reduces the intensity of the radiation, especially at the higher frequencies. In the latter case, the flow noise diffraction mechanism is dominated by the geometry of the tip of the airfoil. When $\omega\delta/U$ is small predictions for $\bar{\theta} \neq 0$ do not depart significantly from the case of a flat airfoil. It is likely, therefore, that, for moderate values of ϵ , the correction to the flat plate results are given to a good approximation by replacing the terms in ϵ in

(6.12) by their respective asymptotic values as $\omega\delta/U \rightarrow \infty$. In that limit (6.12) becomes

$$\frac{c^2 \Phi_2(\omega)}{\rho_0^2 v_*^4 U \delta (a l / |x|^2)} = (C_m h / 12) (U_c / U) \cos^2 \theta [1 + (h v_* / U_c)^2]^{1/2} \\ \times \frac{(\epsilon \delta / s)^{\epsilon/2\pi} (\omega \delta / U_c)^{3-\epsilon/2\pi}}{[(\omega \delta / U_c)^2 + (1 + (h v_* / U_c)^2) / b^2]^2} \left| \frac{1 - (U_s / U_c)^{1+\epsilon/2\pi}}{1 - U_s / U_c} \right|^2. \quad (6.15)$$

Comparisons of predictions of this formula with the results in Figure 5 indicate that the error is less than about 0.25 dB even for ϵ as large as $2\pi/3$ ($\bar{\theta} = 90^\circ$) when $\delta/s = 0.1$. When $\delta/s = 1$, the errors at $\bar{\theta} = 60^\circ, 90^\circ$ exceed 0.5 dB only for $\omega\delta/U \lesssim 2, 6$ respectively. In view of this it is perhaps of interest to note the corresponding asymptotic form of the more general expression (6.8):

$$\Phi_2(\omega) =$$

$$\frac{a l k^2 \cos^2 \theta (\epsilon/s)^{\epsilon/2\pi}}{16 |x|^2} = \int_{-\infty}^{\infty} \frac{P_o(K_1, 0, \omega)}{|K_1|^{1+\epsilon/2\pi}} \left| \frac{1 - (U_s K_1 / \omega)^{1+\epsilon/2\pi}}{1 - U_s K_1 / \omega} \right|^2 dK_1. \quad (6.16)$$

The proportionality exhibited in (6.13) of the spectrum $\Phi_1(\omega)$ of the thickness dipole on ϵ^3 indicates that the contribution to the radiation from this source is small except possibly at the larger values of the included angle $\bar{\theta}$. The ratio s/a of the airfoil thickness to the semi-chord is of order 0.1 - 0.2 in typical experimental configurations [5]. The value of $Z_1(\omega\delta/U_c)$ decreases rapidly with increasing frequency, and this further reduces the significance of $\Phi_1(\omega)$ except when δ/s is large (i.e., for boundary layer flows whose thickness is comparable to the

thickness of the airfoil). The solid curves in Figure 6 illustrate the variation with $\omega\delta/U$ of

$$10 \log_{10} \{ c^2 \phi_1(\omega) / \rho_0^2 v_*^4 U \delta (a \ell / |\underline{x}|^2) \cos^2 \psi \} \text{ (dB)}$$

for $\delta/s = 1$, $s/a = 0.15$, $\bar{\theta} = 30^\circ, 60^\circ, 90^\circ$, and when the remaining flow parameters assume values given previously. For comparison, the dashed curve is the $\bar{\theta} = 90^\circ$ lift dipole spectrum of Figure 5(b). These results suggest that the thickness dipole is negligible except, perhaps, in radiation directions parallel to the airfoil, and when $\bar{\theta} \approx 90^\circ$.

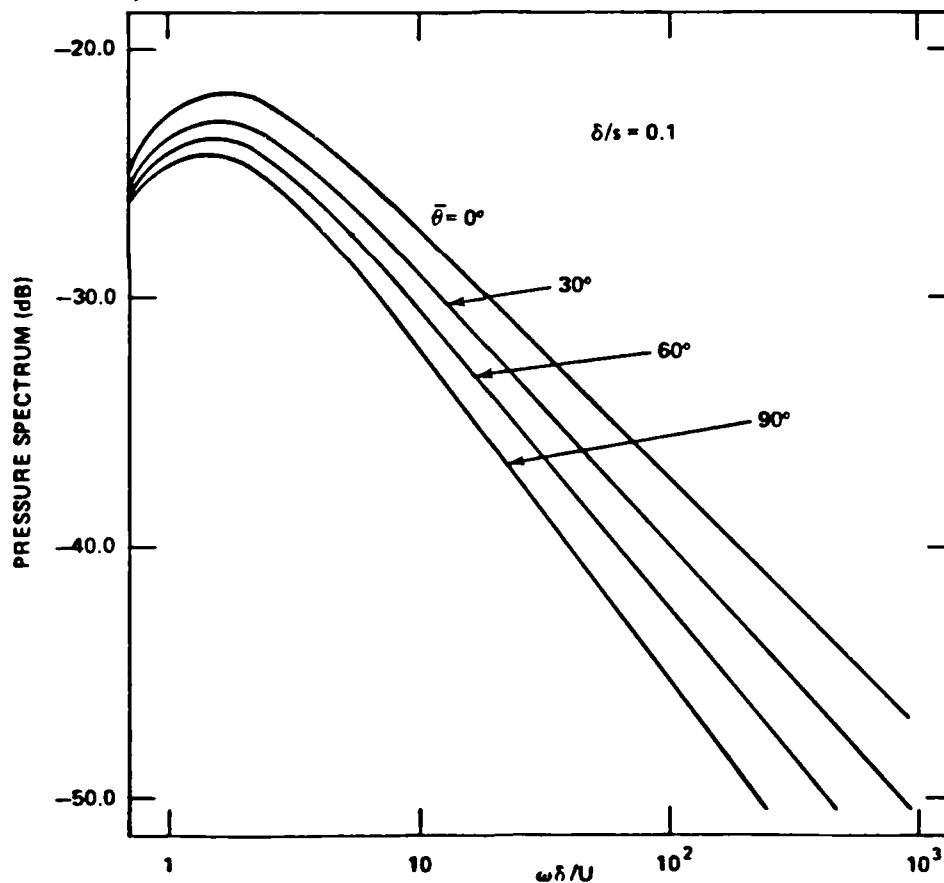


FIGURE 5(a). THE SPECTRUM $10 \log_{10} \{ c^2 \phi_2(\omega) / \rho_0^2 v_*^4 U \delta (a \ell / |\underline{x}|^2) \cos^2 \theta \}$ OF THE LIFT DIPOLE FOR DIFFERENT VALUES OF THE INCLUDED ANGLE $\bar{\theta}$, AND FOR $\delta/s = 0.1$.

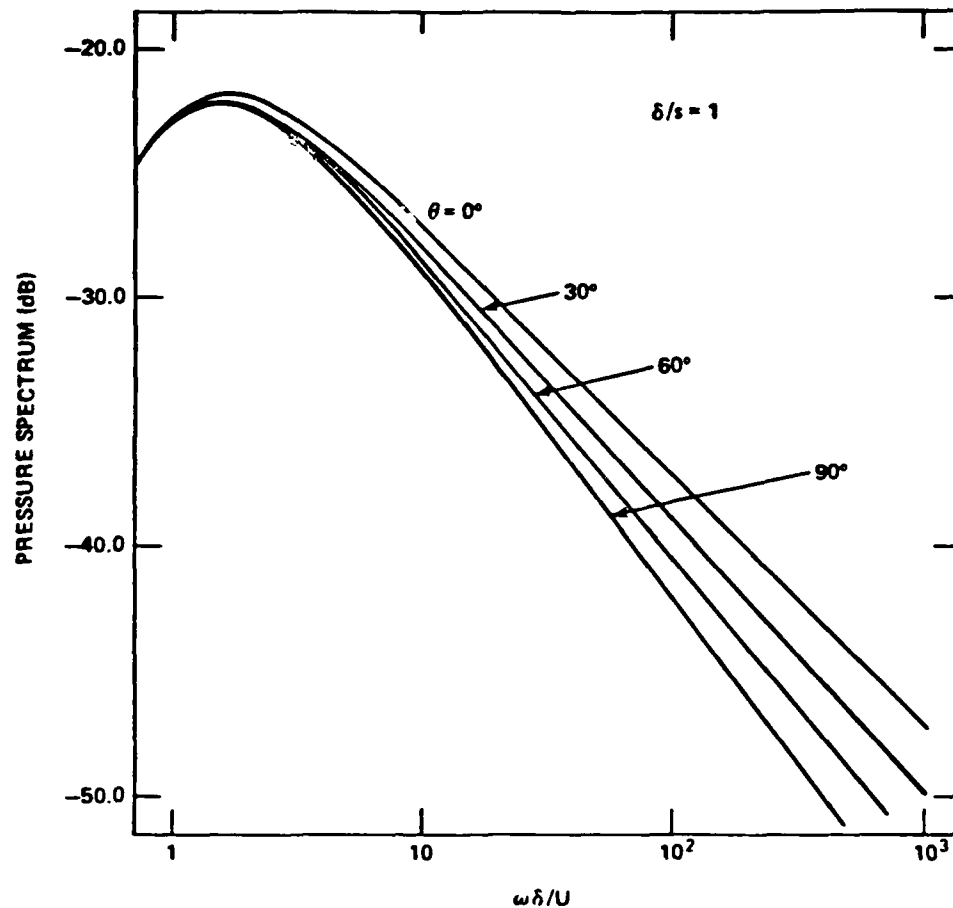


FIGURE 5(b). THE SPECTRUM $10 \cdot \log_{10} \{ c^2 \phi_2(\omega) / \rho_0^2 v_1^2 U \delta (a_1 / |x|^2) \cos^2 \theta \}$ OF THE LIFT DIPOLE FOR DIFFERENT VALUES OF THE INCLUDED ANGLE θ , AND FOR $\delta/s = 1$.

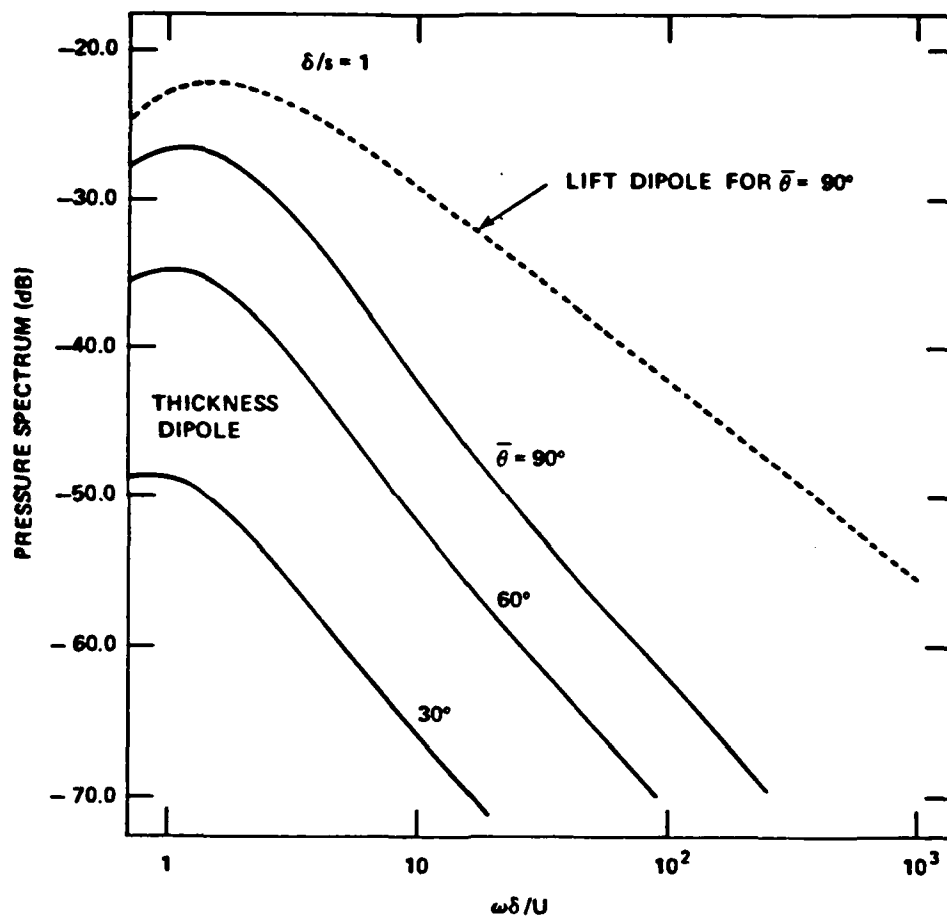


FIGURE 6. THE SPECTRUM $10 \cdot \log_{10} \{ c^2 \phi_1(\omega) / \rho_0^2 v_1^2 U \delta (a_1 / |\underline{x}|^2) \cos^2 \psi \}$ OF THE THICKNESS DIPOLE RADIATION FOR DIFFERENT VALUES OF THE INCLUDED ANGLE $\bar{\theta}$ AND FOR $\delta/s = 1$.

7. DISCUSSION OF THE GENERAL CASE

7.1 Turbulence on the Suction Surface

All of the detailed predictions given in Section 6 are for trailing edge noise produced by turbulent flow in the boundary layer on the lower, "pressure" side of the airfoil. If the included angle $\bar{\theta}$ does not exceed about 30° mean flow separation from the suction surface does not occur [5]. In that case, since the effect on the radiation of the finite included angle $\bar{\theta}$ is important only at the higher frequencies, it can be shown that the formulae of Section 6 remain valid for turbulence convecting past the edge on the suction side of the airfoil. When separation occurs (see Figure 1), turbulent eddies in the suction surface boundary layer which are convected into the trailing edge region from upstream are displaced from the proximity of the edge. It follows that, except when $\omega s/U \ll 1$, their near field pressure fluctuations are exponentially small at the edge. Only the very low frequency, incident boundary layer disturbances can then interact effectively with the trailing edge, and produce sound essentially as for an airfoil of zero thickness.

Turbulence fluctuations within the separated region will, of course, produce high frequency sound by interacting with the edge. If, as seems likely, this turbulence is statistically independent of the boundary layer turbulence on the pressure side, its contribution to the spectrum of the lift dipole radiation may be estimated from the formula

$$\Phi_2(\omega) =$$

$$\frac{a k_o^2 \cos^2 \theta (\epsilon/s)^{\epsilon/2\pi}}{16 |\underline{x}|^2} = \int_{-\infty}^{\infty} \frac{P_s(K_1, 0, \omega)}{|K_1|^{1+\epsilon/2\pi}} \left| \frac{1 - (U_s K_1/\omega)^{1+\epsilon/2\pi}}{1 - U_o K_1/\omega} \right|^2 dK_1 \quad (7.1)$$

provided U_0 denotes the mean flow velocity at the edge of the viscous sublayer. In this expression $P_s(K_1, 0, \omega)$ denotes a local representation of the wall pressure spectrum on the suction side of the airfoil within the separated zone. If it is permissible to assume that the structure of small scale turbulence eddies does not vary significantly in the mean flow direction, the value of $P_s(K_1, 0, \omega)$ may be estimated from measurements of wall pressure at distances exceeding $\sim 1/K_1$ upstream of the trailing edge, at which points the influence on the hydrodynamic pressure field of diffraction at the edge should be small (c.f., [4]). In addition, over a range of intermediate to large mean flow Reynolds number, there will be a pronounced contribution to P_s in the neighborhood of $\omega s/U = 0.5$, $K_1 = \omega/U_0$ corresponding to surface pressure fluctuations caused by large scale, quasiperiodic vortex shedding. In this low frequency case it is necessary to set $\epsilon = 0$ when estimating the radiation from (7.1), or make use of the general formula (6.8).

7.2 Influence of Non-Compactness

It is of interest to note the modifications of the results of this paper when the airfoil has non-compact chord (i.e., for $k_0 a \gg 1$). Attention is confined to the analog of the lift dipole spectrum $\phi_2(\omega)$. The appropriate form of the Green's function can be derived from the results of Section 3 and from the Appendix of reference [8], following which one finds that the principal component of the trailing edge noise is given by

$$\begin{aligned} \phi_2(\omega) &= \frac{2 |k_0| \sin(\bar{\alpha}) \sin^2(\bar{\beta}/2) (\epsilon/s)^{\epsilon/2\pi}}{4\pi |\underline{x}|^2} \\ &\times \int_{-\infty}^{\infty} \frac{P_0(K_1, 0, \omega)}{|K_1|^{1+\epsilon/2\pi}} \left| \frac{1 - (U_s K_1/\omega)^{1+\epsilon/2\pi}}{1 - U_0 K_1/\omega} \right|^2 dK_1, \quad (7.2) \end{aligned}$$

where $\bar{\alpha}$ is the angle between the observer direction \underline{x} and the x_3 -axis (see Figure 7), and $\bar{\beta} = \tan^{-1}(x_2/x_1)$. When $\epsilon = 0$, this expression is equivalent to that given in reference [4] (equation (71) with ϕ_2 identified with $S_K/2$ and P_O with $4\pi K$, and with the neglect of finite Mach number terms) for a half-plane of infinitesimal thickness. In particular, the specific formula (6.15), which is applicable for turbulence on the pressure side of the airfoil, and also on the suction side in the absence of separation, becomes:

$$\frac{c\phi_2(\omega)}{\rho_O^2 v_*^4 \ell (\delta^2/|\underline{x}|^2)} = (C_m h/3\pi) \sin(\bar{\alpha}) \sin^2(\bar{\beta}/2) [1 + (h v_*/U_c)^2]^{1/2} \\ \times \frac{(\epsilon \delta/s)^{\epsilon/2\pi} (\omega \delta/U_c)^{2-\epsilon/2\pi}}{[(\omega \delta/U_c)^2 + (1 + (h v_*/U_c)^2)/b^2]^2} \left| \frac{1 - (U_s/U_c)^{1+\epsilon/2\pi}}{1 - U_s/U_O} \right|^2 \quad (7.3)$$

The principal difference between (7.1), (7.2) is the reduction from quadratic to linear dependence of $\phi_2(\omega)$ on k_O . This implies that the overall intensity of the trailing edge noise is proportional to $\rho_O U^3 M^2$ for a non-compact airfoil, as opposed to $\rho_O U^3 M^3$ for the compact airfoil [1].

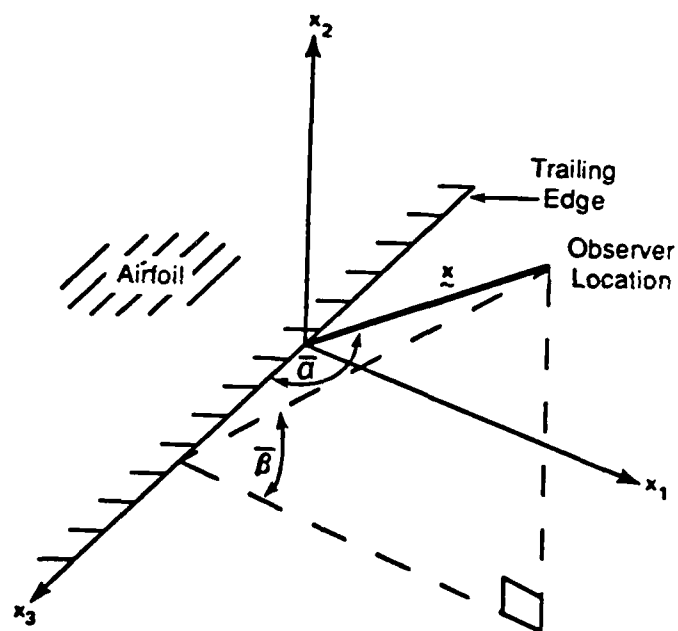


FIGURE 7. COORDINATES DEFINING THE RADIATION FROM AN AIRFOIL OF NON-COMPACT CHORD.

8. CONCLUSION

There are two principal components of the sound produced by low Mach number turbulent flow over a beveled, or asymmetrically rounded, trailing edge. These can be identified with hydro-acoustic sources of dipole type associated with the fluctuations in the lift and with the finite thickness of the airfoil. The influence of beveling on the lift dipole is significant only at sufficiently high frequency that the trailing edge region of the airfoil can be regarded as a straight-sided wedge over distances of the order of the length scale of the turbulence. In that case, the spectrum of the dipole radiation falls below that for a trailing edge of zero included angle (i.e., for a thin plate airfoil) by an amount which increases progressively with frequency. The radiation generated by the thickness dipole is absent in conventional treatments of trailing edge noise. For an airfoil of compact chord its intensity varies approximately as the cube of the included angle and linearly as the airfoil thickness, and is generally negligible except possibly at low frequencies, for trailing edges of large included angle, and in radiation directions lying in the mean plane of the airfoil.

REFERENCES

1. J.E. Ffowcs Williams and L.H. Hall 1970 J. Fluid Mech. 40, 657-670. Aerodynamic sound generation by turbulent flow near a scattering half-plane.
2. D.M. Chase 1972 J. Acoust. Soc. Am. 52, 1011-1023. Sound radiated by turbulent flow off a rigid half-plane as obtained from a wavevector spectrum of hydrodynamic pressure.
3. K.I. Chandiramani 1974 J. Acoust. Soc. Am. 55, 19-29. Diffraction of evanescent waves with applications to aerodynamically scattered sound and radiation from un baffled plates.
4. M.S. Howe 1978 J. Sound Vib. 61, 437-465. A review of the theory of trailing edge noise.
5. W.K. Blake 1983 Excitation of plates and hydrofoils by trailing edge flows. In Turbulence-Induced Vibrations and Noise of Structures (ed. M.M. Sevik). New York: ASME.
6. W.K. Blake 1984 Aero-Hydroacoustics for Ships. David Taylor Naval Ship Research and Development Center Report No. 84/010.
7. M.S. Howe 1979 Diffraction of Evanescent Waves by a Wedge. BBN Technical Memorandum No. 509.
8. M.S. Howe 1975 J. Fluid Mech. 71, 625-673. Contributions to the theory of aerodynamic sound, with application to excess jet noise and the theory of the flute.
9. J.A. Stratton 1941 Electromagnetic Theory. New York: McGraw-Hill.
10. N. Curle 1955 Proc. Roy. Soc. Lond. A231, 505-514. The influence of solid boundaries upon aerodynamic sound.
11. L.M. Milne-Thomson 1968 Theoretical Hydrodynamics (5th edition). London: MacMillan.
12. Th. von Karman and W.R. Sears 1938 J. Aero. Sciences 5, 379-390. Airfoil theory for non-uniform motion.

END

DATE

FILMED

6-1988

DTic